Third International Symposium on the Effects of Surface Geology on Seismic Motion
Grenoble, France, 30 August - 1 September 2006
Paper Number: xxx

3D SPECTRAL ELEMENT METHOD SIMULATIONS OF THE SEISMIC RESPONSE IN THE CARACAS BASIN

Elise DELAVAUD[1], Paul CUPILLARD[1], Gaetano FESTA[1], Jean-Pierre VILOTTE[1]
1 Equipe de Sismologie, Institut de Physique du Globe, Paris, France

ABSTRACT - This paper presents the first results of 3D simulations of the seismic response in the Caracas basin using the spectral element method. The seismic response of the basin is obtained by the excitation of an incident plane wave which is efficiently implemented via its traction and velocity at the rock sediments interface. A generalized filtering perfectly matched layer allows for a better absorption of surface waves in elongated basins. Our simulations clearly show combined effects from the topography and the basin, with diffracted waves coming from the mountains, and low frequency energy trapped in the deepest part of the basin. Spectral ratio exhibits focalization and 3D amplification effects.

1. Introduction

3D simulation presents challenges for assessing the seismic response of heterogeneous media with topography and internal interfaces, such as sedimentary basins. In such models, where most of the energy is transported by diffracted waves, the 3D geometry and the local geological features can result in significant amplifications and trapping of specific frequencies. These 3D effects must be taken into account for strong motion prediction and seismic risk assessment and illustrate the need for detailed models, and flexible numerical techniques (Sanchez-Sesma et al., 1996).

Many techniques have been developed to model elastic-wave propagation. The finite-difference methods have been widely used for smooth and steep topography (Olsen, 2000). Despite some recent improvements, they suffer from serious limitations, in particular when it comes to accurate computation of surface waves and the handling of complex geometries and strong heterogeneities. The spectral element method (SEM), introduced in seismology ten years ago (Komatitsch and Vilotte, 1998) is a high-order variational technique that has already proven to be a powerful tool at regional (Komatitsch et al., 2004) and global scales (Capdeville et al., 2003; Chaljub et al., 2003). It provides solutions to the increasing demand for geometrical flexibility and for accuracy for both body and surface waves. The SEM is well adapted to tackle problems linked to the seismic response in heterogeneous media like basins. It exhibits a high accuracy, in particular for the resolution of surface waves, and the interaction between body waves and the topography of the main geological discontinuities.

Caracas is built on a typical alluvium basin and bordered by a strong topographic barrier, the Avila mountain range. It has been the subject of many studies since site effects have been revealed during the 1967 Mw=6.6 Caracas earthquake (Bolton Seed et al., 1972). Geological observations, drill holes, seismic surveys and gravimetric measurements have been recently re-analyzed to provide, with new seismic refraction

profiles done by FUNVISIS in 2001, a reliable model of the basin for the sediments' thickness and velocity.

This paper describes first new developments of the SEM used for the modeling of the seismic response in basins, a generalized filtering perfectly matched layer for a better absorption of surface waves and an efficient implementation of incident plane waves. The difficulties associated with unstructured mesh generation, the most problematic aspect of the modeling process, are discussed further.

2. Numerical technique

The SEM is a high order method based on the approximation of the variational formulation of elastodynamics. A domain is decomposed into hexahedral finite elements, mapped on a reference cube where Gauss Lobatto Legendre points (GLL) are defined. The wave field is represented in terms of high-degree Lagrange polynomials on the GLL interpolation points. The choice of a quadrature rule at the same GLL points results in a diagonal mass matrix, allowing for an explicit time integration Newmark scheme. The system solved at each time step can be written as follows

$$\begin{aligned} V^{n+1} &= V^n + \Delta t M^{-1}(F^{ext,n+1/2} - F^{\text{int}}(U^{n+1/2}) + B^T \lambda^{n+1/2}) \\ U^{n+1} &= U^n + \Delta t V^{n+1/2} \end{aligned} \qquad (1)$$

where U and V denote the vectors containing the displacement and the velocity at all the nodes, and λ the traction defined only at the interfaces where a Neumann condition is imposed, B^T being an interface matrix. M is the diagonal mass matrix, F^{ext} and F^{int} external and internal forces, respectively. Superscript n stands for the time step.

Due to the geometrical flexibility the SEM shares with finite-element methods, it can handle complex geometries with an unstructured mesh, which respects the main discontinuities and topological features. Special attention should be paid to the mesh generation. Through the Courant number, the time step is linked to the space discretization and can become tremendously small if the mesh contains small or exceptionally deformed elements. This situation is frequently found when dealing with rough interfaces and topography. Deformed elements should be especially avoided as the effect of jacobian high variations on the numerical accuracy is not well known.

2.1. Generalized Filtering Perfectly Matched Layer

When modeling low frequencies in thin media such as basins, instabilities can arise from the interaction between propagating evanescent waves and the perfectly matched layer (PML) used as absorbing boundary condition at the bottom of the model. These effects come from the surface waves which have lost their characteristic exponential feature in the standard PML (Festa and Vilotte, 2005; Festa et al., 2005). In very long simulations, these instabilities affect the total volume, and can significantly pollute the records even at the free surface. To avoid this problem, the bottom of the model should be put at a sufficient depth, but it will increase the computational cost. A modification of the PML by adding a cut-off and an overdamping enables the evanescent wave characteristics for low frequencies in these layers to be preserved without producing any spurious effect. The computational domain size can be thus optimized and calculation costs reduced.

2.2. Plane wave implementation

The seismic response in the basin is assessed through an incident plane wave excitation. It is usually introduced as an initial condition, but this classical implementation exhibits inconveniences. The coupling between this initial condition and the absorbing conditions imposed at the borders of the model can produce diffraction phenomena. Moreover, the computational domain needs to be enlarged compared to the domain of interest when an inclined wave is considered. We introduce an incident plane wave with the SEM directly at the rock sediments interface and at the free surface of the rock part. A decomposition technique is applied: the elastodynamic equation is separately solved in both domains, but not on the same fields.

- In the rock, the wave is decomposed into an incident, analytically known, wave field and into a diffracted wave field which is numerically calculated.
- In the sediments, total field is computed.
- Communication between the domains is insured at the rock sediments interface (Γ) by a continuity condition on the velocities and the tractions.

This strategy leads to the following system of equations

$$\begin{aligned} V_d^{r,n+1} &= V_d^{r,n} + \Delta t (M^r)^{-1} (-F(U_d^{r,n+1/2}) + B^T \lambda_d^{r,n+1/2}) \\ V^{s,n+1} &= V^{s,n} + \Delta t (M^s)^{-1} (-F^{\text{int}}(U^{s,n+1/2}) - B^T \lambda^{s,n+1/2}) \\ V_i^{r,n+1} &= V^{s,n+1} - V_d^{r,n+1} \quad on\ \Gamma \\ B^T \lambda^{s,n+1/2} &= B^T \lambda_d^{r,n+1/2} + B^T \lambda_i^{r,n+1/2} \quad on\ \Gamma \end{aligned} \tag{2}$$

where r and s superscripts stand for rock and sediments, i and d indexes for incident and diffracted fields, respectively. For the rock domain, F contains the internal forces and the contribution of the incident wave at the free surface.

The complete solution is retrieved by adding the analytical part. Propagation of the incoming wave field is thus avoided, suppressing spurious effects at the boundaries. The restriction of the calculation domain to the study area allows for a gain in computation time.

3. Seismic response in the Caracas basin

3.1 Caracas basin

The city of Caracas is located about 13km from the coast of northern Venezuela in an alluvial valley of the coastal mountains. The Caracas basin is narrow, long and almost flat, about 25km long in east-west direction and 3-4km wide, bordered to the north by a formidable topographic barrier, the Avila mountain range, and to the south by smaller hills. Alluvium materials like sand, gravel and stiff clay have been deposited by the Guaire River and alluvial fans coming from the Avila range.

The major seismic activity comes from a strike slip fault system associated with the movement along the Caribbean-South America plate boundary zone. During the 1967 magnitude Mw=6.6 Caracas earthquake, which occurred 25km northwest of the city, four buildings collapsed and 300 people were killed. Strong site effects were revealed and in particular, a close relationship between the building damage and the soil thickness was established. Following this event, various studies have been carried out to characterize the structure of the Caracas basin. A reliable subsurface model is now available thanks to

recent geological and geophysical investigations. A total of 166 drill holes, seismic refraction results (Weston, 1969), and gravimetric measurements were re-analyzed (Kantak et al., 2002). In order to provide more data on the sedimentary thickness and seismic velocities, seismic refraction measurements were carried out in the region of study by FUNVISIS in July 2001 (Sánchez and Schmitz, 2002).

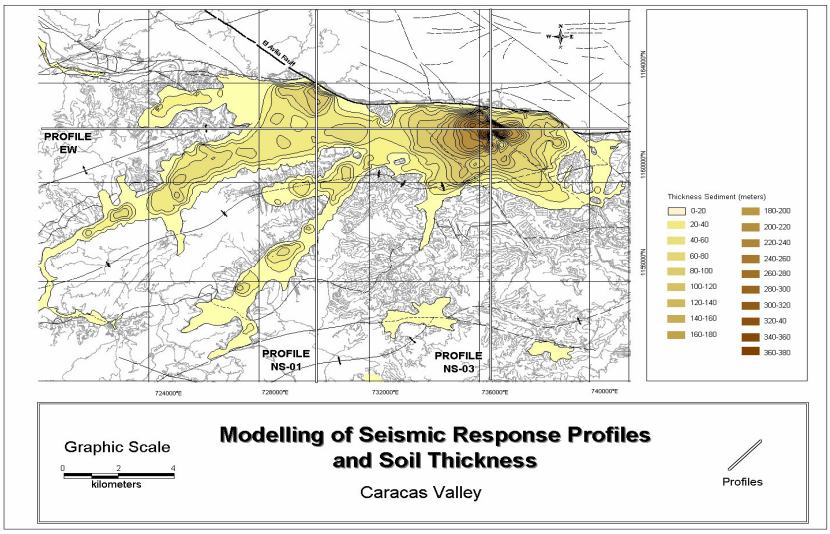

Figure 1. Map of sediment thickness in the Caracas valley based on geological observations, drill holes and geophysical data (Weston, 1969; Kantak et al., 2002; Sánchez and Schmitz, 2002).

In Figure 1, the two north-south profiles correspond to the areas where the damage in the 1967 earthquake was concentrated: San Bernardino (SB), profile NS-01 and Los Palos Grandes (LPG), profile NS-03. They coincide with the deepest parts of the basin, about 100m for SB and 320m for LPG. To assess the fundamental periods of vibration within the valley, microtremors have been measured during the 1990's (Abeki et al., 1998; Duval et al., 2001) using either the Nakamura method or H/V ratio. This data has been recently densified in a 250m grid. Predominant periods derived from H/V ratio correlate well with the 1D sediment thicknesses, the highest values corresponding to the two deepest regions, SB and LPG, with periods of about 1s and 2s, respectively. The data we used for our simulations has been supplied by FUNVISIS.

The city of Caracas continues to grow. New construction within the valley and a recent urbanization along the slopes increase the need for a precise microzonation and risk assessment. 2D simulations along the LPG profile (Semblat et al., 2002) show strong amplifications in the deepest part of the alluvial deposit at low frequencies and further away from it for higher frequencies. 3D simulations are attempting to evaluate the importance of 3D effects (amplification, focalization and interference phenomena) on the seismic response coming from the geological and geometrical features of the basin, the surrounding steep topography and their mutual interaction.

3.2. Basin model

For the simulations, we selected a volume of 23km long (east-west direction), 17km wide (north-south direction) with a maximum 4.5km height, including the Avila mountain range and the hills in the south. The 3D unstructured mesh generation remains a difficult part of the modeling process. Even though mesh generators like CUBIT offer new perspectives, assessing the quality of an unstructured hexahedral mesh both in terms of geometrical and numerical accuracy is still a serious challenge. As a first step we simplified the basin

Table I. velocities and densities in the basin model

	P velocity	S velocity	density
Sediments	2300 m/s	850 m/s	2400 kg/m^3
Rock	3800 m/s	2200 m/s	2700 kg/m^3

structure, shape and velocity. Shallow parts of less than 30m as well as some secondary basins haven't been incorporated, and basin edges have been cut at a depth of 70m (Figure 2). These simplifications are reasonable for the low frequency simulations we made where 70m corresponds to a 1D fundamental frequency of 3Hz. No anelastic attenuation is taken into account, and homogeneous velocities in the rock and sediments are considered (Table I).

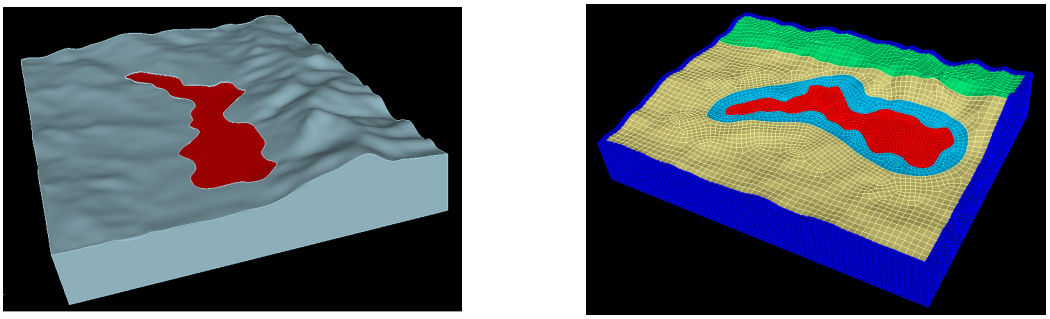

Figure 2. On the left, the 3D model used for our simulations. The basin is in red. On the right, the unstructured mesh realized with CUBIT (colors outside the basin correspond to an artificial cut for controlling the elements size).

The unstructured mesh composed of 38394 elements was generated with CUBIT (Figure 2). It respects the steep topography and the velocity discontinuities with a conforming coarsening from the basin to the external boundaries of the model. Our 3D code is a MPI parallel version. Simulations were made with a polynomial degree of 6, with a time step of 0.6ms corresponding to a Courant number of 0.2. A 1s signal simulation was obtained in about 1h elapsed time on 16 Opteron 256 processors.

3.3 3D simulations

We studied the basin response through its excitation by a north-south polarized plane S wave with a 1Hz central frequency. Polarization and frequency correspond to the case of maximum amplification for a 3D Gaussian shape hill (Komatitsch et al., 1998). The effects from the topography and the basin can be clearly observed. We focused in particular on the SB and LPG profiles (Figure 3).

The topographic effects are characterized by an amplification of motion on the mountain and diffracted waves being composed of a surface P wave traveling below the surface and a Rayleigh wave. The basin effects consist of trapping and amplification of the wave field in the basin, which produce more complex and longer signals. This basin effect is stronger in LPG where sediments are deeper. Most of the energy remains here due to amplified 2D and 3D focusing effects.

A 3D visualization of the velocity field modulus exhibits both 2D and 3D effects from the mountain. A P wave front parallel to the major axis travels firstly from the top of the topography towards the basin then Rayleigh waves follow, and focus in the LPG area.

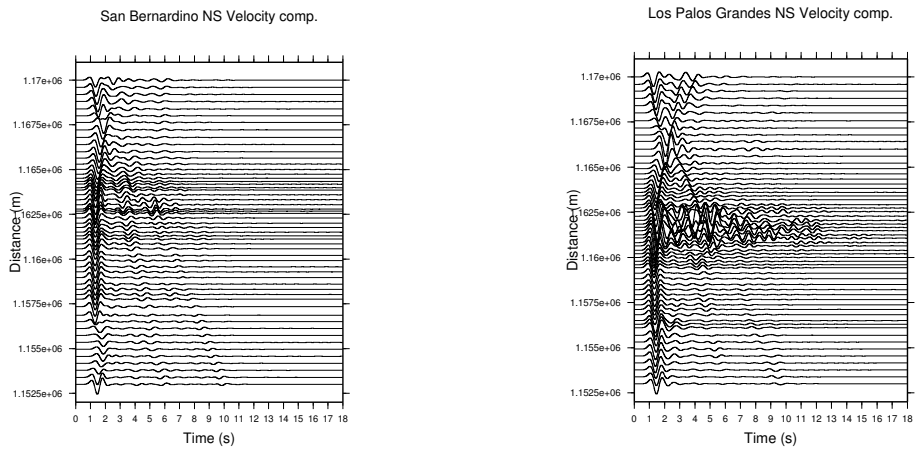

Figure 3. NS velocity component due to a NS polarized plane S wave along SB and LPG profiles.

The Spectral ratio (SR), defined as the ratio of the Fourier amplitude spectrum of the observed movement at the surface with the incident one, is presented along the LPG profile and for the entire basin (Figure 4). Looking at the entire LPG profile, the highest amplifications are clearly localized in the basin. The influence of the topography is negligible compared to the effects of the basin, even if a small peak at the top of the mountain can be noticed. Frequency peaks follow well the thickness of the sediments: the associated frequency value increases as the sediments depth decreases. The deepest part shows an amplification at around 0.8Hz (the 1D fundamental frequency associated to our velocity model is 0.66Hz). Amplifications can be then observed at the borders of the basin, corresponding to higher frequencies. These observations correlate well with the H/V ratio results on microtremor found by Duval et al. (2001). Other amplification peaks can be found along the profile as a consequence of 2D/3D focusing effects.

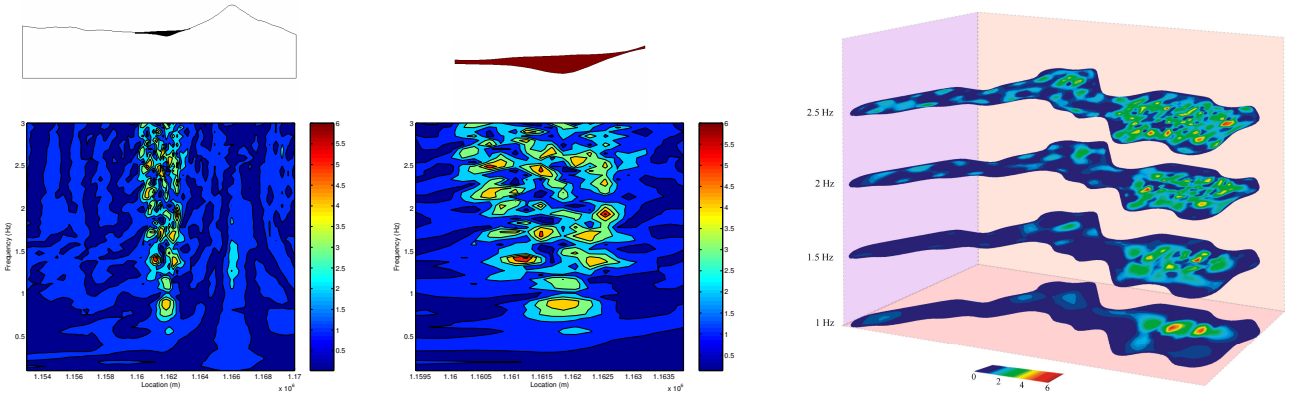

Figure 4. Spectral ratio for the NS velocity component due to a NS polarized plane S wave, along the LPG profile including the topography (left), along the LPG profile restricted to the basin section (middle) and for the entire basin for frequencies from 1 to 2.5Hz (right).

SR results for the total basin show that up to 2.5Hz, the highest amplifications are concentrated in the deepest part of the basin, the LPG area. A clear amplification is observed at 1Hz, then thicker parts are excited at higher frequencies. Above 1.5Hz, localized peaks reveal 2D/3D effects. At these frequencies, amplifications also occur in the SB area and interactions with the east part of the basin are expected.

4. Conclusions

We have presented an application of 3D SEM simulations of the seismic response in the Caracas valley. These have been carried out on an unstructured mesh taking into account the regional topography and the basin geometry. Given the limitations of the low frequency simplified model we considered, we observed 2D and 3D geometrical effects. Diffracted waves are generated by the mountain topography going into the basin, where high amplifications occur in the deepest area. Focusing effects are also observed in thicker sections at higher frequencies. This first step provides encouraging results for further simulations based on a more realistic model in terms of geometry, velocity structures and anelastic attenuation. A scenario study depending on the incidence, polarization and time function of the source at frequencies up to 5Hz should enable us to analyze and evaluate more precisely the 3D effects. An ongoing work aims to quantify the geometrical heterogeneity of the unstructured mesh and its influence in time and space on the numerical resolution.

5. References

Abeki, N., K. Seo, I. Matsuda, T. Enomoto, D. Watanabe, M. Schmitz, H. Rendón, and J. Sánchez (1998). Microtremor observations in Caracas city, Venezuela. *In Irikura et al., Editors. The effects of surface Geology on Seismic Motion, Rotterdam, AA Balkema*, 619-624.

Bolton Seed, H., R. V. Whitman, H. Dezfulian, R. Dobry, and I. M. Idriss (1972). Relationships between soil conditions and building damage in the 1967 Caracas Earthquake. *Journal of the Soil Mechanics and Foundations Division* 98(8), 787-806.

Capdeville, Y., E. Chaljub, J. P. Vilotte, and J. P. Montagner (2003). Coupling the spectral element method with a modal solution for elastic wave propagation in global Earth models. *Geophysical Journal International* 152, 34-67.

Chaljub, E., Y. Capdeville, and J. P. Vilotte (2003). Solving elastodynamics in a fluid-solid heterogeneous sphere: a parallel spectral element approximation on non-conforming grids. *Journal of Computational Physics 187(*(2), 457-491.

Duval, A. M., S. Vidal, J. P. Méneroud, A. Singer, F. De Santis, C. Ramos, G. Romero, R. Rodriguez, A. Pernia, N. Reyes, and C. Griman (2001). Caracas, Venezuela, Site Effect Determination with Microtremors. *Pure and Applied Geophysics* 158, 2513-2523.

Festa, G., and J. P. Vilotte (2005). The Newmark scheme as a velocity-stress time-staggering: an efficient PML implementation for spectral element simulations of elastodynamics. *Geophysical Journal International* 161(3), 789-812.

Festa, G., E. Delavaud, and J. P. Vilotte (2005). Interaction between surface waves and absorbing boundaries for wave propagation in geological basins: 2D numerical simulations. *Geophysical Research Letters* 32(20), L20306.

Kantak, P., M. Schmitz, and F. Audemard (2002). Perfil geológico longitudinal al valle de Caracas, con énfasis en los sedimentos más recientes, para fines de microzonificación sísmica. *III Coloquio sobre Microzonificación Sísmica*, Memorias, Serie Técnica No. 1 – 2002, FUNVISIS, Caracas, 56-58.

Komatitsch, D., and J. P. Vilotte (1998). The spectral-element method: an efficient tool to simulate the seismic response of 2D and 3D geological structures. *Bulletin of the Seismological Society of America* 88(2), 368-392.

Komatitsch, D., Q. Liu, J. Tromp, P. Süss, C. Stidham, and J. H. Shaw (2004). Simulations of ground motion in the Los Angeles basin based upon the spectral-element method. *Bulletin of the Seismological Society of America* 94, 187-206.

Olsen, K. B. (2000). Site amplification in the Los Angeles basin from three-dimensional modeling of ground motion. *Bulletin of the Seismological Society of America* 90, S77-S94.

Sanchez-Sesma, F.J., R. Bentes, and J. Bielak (1996). The assessment of strong ground motion: What lies ahead? *Proceedings of the 11th World Conference on Earthquake Engineering, Acapulco, Mexico*. Paper No 2014.

Sánchez, J., and M. Schmitz (2002). Mediciones sísmica profundas y gravimétricas en Caracas para la determinación del espesor de sedimentos y velocidades sísmica como aporte para el estudio de Microzonificación Sísmica. *XI Congreso Venezolano de Geofísica, Caracas*.

Semblat, J. F., A. M. Duval and P. Dangla (2002). Seismic site effects in a deep alluvial basin : numerical analysis by the boundary element method. *Computers and Geotechnics* 29(7), 573-585.

Weston Inc. (1969). Seismic Investigations in the valley of Caracas and the Lithoral Central. *Weston Geophysical Engineers International, Inc*.